



Met23Lys mutation in subunit gamma of F_0F_1 -ATP synthase from *Rhodobacter capsulatus* impairs the activation of ATP hydrolysis by protonmotive force

Boris A. Feniouk^{a,*}, Alberto Rebecchi^b, Donatella Giovannini^b, Sofie Anefors^{a,b,1}, Armen Y. Mulikidjanian^{a,c,2}, Wolfgang Junge^a, Paola Turina^b, B. Andrea Melandri^b

^a Division of Biophysics, School of Biology/Chemistry, University of Osnabrück, D-49069 Osnabrück, Germany

^b Department of Biology, Lab. of Biochemistry and Biophysics, University of Bologna, 40126 Bologna, Italy

^c A.N.Belozersky Institute of Physico-Chemical Biology, Moscow State University, 119899, Moscow, Russia

Received 25 May 2007; received in revised form 18 July 2007; accepted 19 July 2007

Abstract

H^+ - F_0F_1 -ATP synthase couples proton flow through its membrane portion, F_0 , to the synthesis of ATP in its headpiece, F_1 . Upon reversal of the reaction the enzyme functions as a proton pumping ATPase. Even in the simplest bacterial enzyme the ATPase activity is regulated by several mechanisms, involving inhibition by MgADP, conformational transitions of the ϵ subunit, and activation by protonmotive force. Here we report that the Met23Lys mutation in the γ subunit of the *Rhodobacter capsulatus* ATP synthase significantly impaired the activation of ATP hydrolysis by protonmotive force. The impairment in the mutant was presumably due to the faster enzyme deactivation that was particularly evident at low ATP/ADP ratio. We suggest that the electrostatic interaction of the introduced γ Lys23 with the DELSEED region of subunit β stabilized the ADP-inhibited state of the enzyme by hindering the rotation of subunit γ rotation which is necessary for the activation.

© 2007 Elsevier B.V. All rights reserved.

Keywords: ATP synthase; Subunit gamma; ADP inhibition; Activation; Met23Lys; *Rhodobacter capsulatus*

1. Introduction

H^+ transporting F_0F_1 -ATP synthase (F_0F_1 -complex) catalyses ATP synthesis/hydrolysis that is coupled to transmembrane proton transport. F_0F_1 is present in the inner membranes of mito-

chondria, thylakoid membranes of chloroplasts and bacterial plasma membranes. Enzymes from different organisms show strikingly high structural and functional homology and presumably have the same catalytic mechanism.

F_0F_1 -ATP synthase is composed of two distinct portions connected by two “stalks”. The hydrophilic F_1 -portion (in the simplest bacterial enzyme a complex of five types of subunits in stoichiometry $\alpha_3\beta_3\gamma_1\delta_1\epsilon_1$) protrudes by ~ 100 Å from the membrane and is responsible for ATP synthesis/hydrolysis. The larger α and β subunits form a hexamer with elongated subunit γ inside it. The hydrophobic F_0 -portion (in most bacteria a complex of three types of subunits in stoichiometry $a_1b_2c_{\sim 10}$) is embedded into the membrane and translocates protons. One of the two stalks mentioned above is composed by centrally located $\gamma\epsilon$ -subunits complex bound to c -subunits oligomer. Another one is formed by peripheral b_2 -dimer (bb' heterodimer in case of *Rhodobacter capsulatus*) that connects subunit a to the $\alpha_3\beta_3\delta$ -complex (see [1–4] for reviews on the F_0F_1 structure).

Abbreviations: F_0F_1 , H^+ transporting F_0F_1 -ATP synthase; $\Delta\psi$, transmembrane difference of proton electrochemical potential; $\Delta\psi$, transmembrane difference of electrical potential; BChl, bacteriochlorophyll; ACMA, 9-amino-6-chloro-2-methoxy-acrydine

* Corresponding author. Present address: ICORP ATP-Synthesis Regulation Project (Japanese Science and Technology Agency), National Museum of Emerging Science and Innovation, 2-41 Aomi, Koto-ku, Tokyo 135-0064, Japan. Tel.: +81 3 3570 9186; fax: +81 3 3570 9187.

E-mail address: feniouk[at]atp.miraikan.jst.go.jp (B.A. Feniouk).

¹ Present address: Unite de Biologie et Genetique du Paludisme, Institute Pasteur, 25-28 rue du Dr Roux, 75724 Paris, France.

² Present address: School of Physics, University of Osnabrück, D-49069 Osnabrück, Germany.

46 A unique feature of the enzyme is the rotary catalysis [5–7].
 47 During ATP synthesis proton transport through F_O drives the
 48 rotation of $\gamma_1\epsilon_1c_{\sim 10}$ -complex (so called “rotor”) relative to the
 49 rest of the enzyme, or “stator” $\alpha_3\beta_3\delta_1a_1b_2$ (see [8–13] for recent
 50 reviews).

51 The details of energy transmission between the catalytic F_1 -
 52 portion and the proton transporting F_O are not fully understood.
 53 One of the main reasons for that is the complex regulation of the
 54 ATP synthase. A well-known regulatory feature of ATP synthase
 55 is inhibition of its ATPase activity by ADP. It is demonstrated
 56 that the binding (or failure to release) of MgADP at the high
 57 affinity catalytic site inactivates the enzyme in terms of ATP
 58 hydrolysis [14–21]. Upon the energization of the membrane, the
 59 tightly bound ADP is released from the F_1 -portion [22–25].
 60 Several studies on bacterial, chloroplast and mitochondrial F_OF_1
 61 have shown that after membrane energization the ATPase
 62 activity of the enzyme increased markedly [26–32], suggesting
 63 that release of the tightly bound ADP relieves the inhibition.

64 In this work we have further investigated the activation of ATP
 65 hydrolysis in F_OF_1 of the photoheterotrophic bacteria *Rb.*
 66 *capsulatus* that was induced by transmembrane proton electro-
 67 chemical potential difference ($\Delta\tilde{\mu}_H^+$). Isolated membrane vesicles
 68 (chromatophores) derived from these bacteria contain complete
 69 photosynthetic electron transport chain and F_OF_1 . The important
 70 advantages of chromatophores are: (1) $\Delta\tilde{\mu}_H^+$ can be generated by
 71 light; transmembrane voltage ($\Delta\psi$) jumps of up to ≈ 100 mV can
 72 be achieved in a few milliseconds if a short flash of light is used for
 73 excitation; (2) voltage transients and thereby transmembrane
 74 charge transfer can be monitored with high time resolution by the
 75 electrochromic absorption band shift of intrinsic carotenoid
 76 pigments [33,34]; (3) the electrical ($\Delta\psi$) or the chemical (ΔpH)
 77 components of the $\Delta\tilde{\mu}_H^+$ can be selectively switched off by
 78 appropriate ionophores; (4) it is possible to prepare very small
 79 chromatophore vesicles (average diameter of approximately
 80 30 nm) [34] that contain less than one active F_OF_1 per vesicle
 81 on average, which allows a “single molecule per vesicle” study
 82 [34,35].

83 Taking advantage of these favorable features, we investigat-
 84 ed the activation of ATP hydrolysis in *Rb. capsulatus* wild-type
 85 F_OF_1 and in the mutated enzyme with γMet23 changed to Lys.

86 This mutation has been studied previously in the *Escherichia*
 87 *coli* enzyme where it was shown to affect coupling between ATP
 88 hydrolysis and proton transport, while slightly impairing catalysis
 89 [36,37]. The mutation was proposed to introduce extra electro-
 90 static interactions between γLys23 and βGlu381 in the
 91 $^{380}\text{DELSEED}^{386}$ segment of the β subunit [38,39]. However,
 92 the ATP induced rotation of γ -subunit in the purified F_1 -portion
 93 (as detected with an attached actin filament providing a heavy
 94 viscous load) was undistinguishable in the mutant and in the wild-
 95 type enzyme [40]. The author concluded that the uncoupling was
 96 likely to occur at the interface between F_1 and F_O .

97 In this work we report that the activation of ATP hydrolysis by
 98 $\Delta\tilde{\mu}_H^+$ was severely impaired in the mutant enzyme. To our
 99 knowledge, this is the first experimental demonstration that a
 100 single amino acid substitution might affect such activation. Our
 101 data indicate that the rotation of subunit γ might play an important
 102 role in activation of ATP hydrolysis by $\Delta\tilde{\mu}_H^+$.

2. Materials and methods

2.1. Cell growth and chromatophores preparation

105 *Rb. capsulatus* B100 strain was grown photoheterotrophically in a synthetic
 106 medium (RCV medium containing malate as a carbon source) [41] as described
 107 previously [35]. In case of the strains with introduced pRK415 plasmid, kanamycin
 108 and tetracycline were added to the medium to the final concentrations of 25 mg/
 109 l and 2 mg/l, respectively. Chromatophores were prepared by sonication with high
 110 output power to yield smaller vesicles (average diameter of ≈ 30 nm) as in [34].
 111 French-press treatment was used instead of sonication for preparation of
 112 chromatophores used in experiments presented in Figs. 1, 7 and 8. In the latter

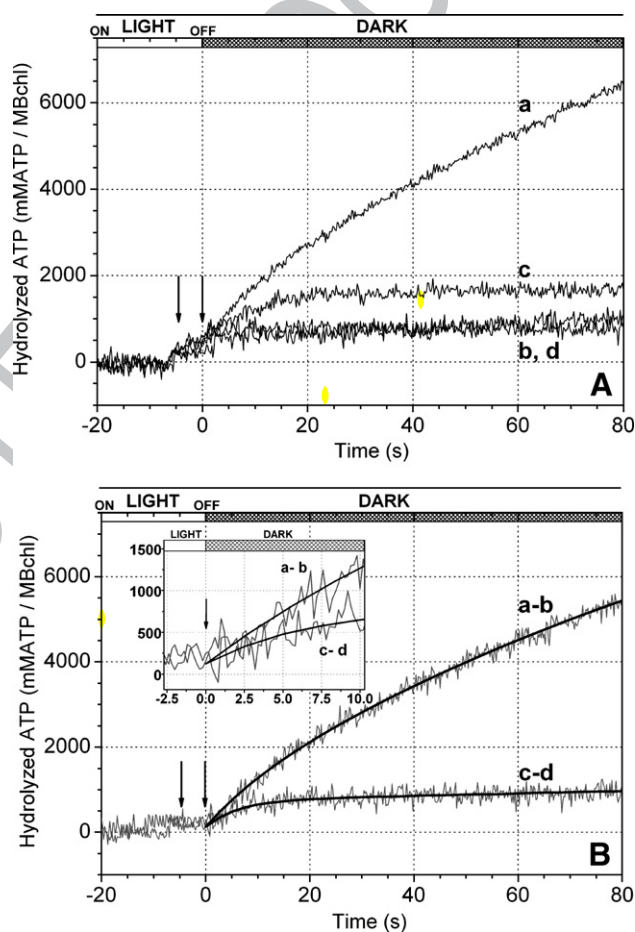


Fig. 1. Activation of ATP hydrolysis by $\Delta\tilde{\mu}_H^+$ in chromatophores of *Rb. capsulatus* wild-type and $\gamma\text{Met23Lys}$ mutant. Changes of ATP concentrations were monitored by Phenol Red absorption changes as described in Materials and methods. The chromatophores suspension ($10 \mu\text{M Bechl}$) in the cuvette was illuminated for 30 s. After 25 s of illumination 1 mM ATP was added (first arrow) and after additional 5 s (second arrow) the light was switched off and at the same time uncouplers ($0.4 \mu\text{M}$ nigericin and valinomycin) were added. Traces have been corrected for dilution and for the small absorption change following the pH change due to ATP addition. (Panel A) Trace a—wild type chromatophores, no inhibitors; trace b—wild type chromatophores, $20 \mu\text{g/ml}$ oligomycin; trace c— $\gamma\text{Met23Lys}$ mutant chromatophores, no inhibitors; trace d— $\gamma\text{Met23Lys}$ mutant chromatophores, $20 \mu\text{g/ml}$ oligomycin. Each trace is an average of two measurements. (Panel B) To reveal the oligomycin-sensitive activity, the traces obtained in the presence of oligomycin have been subtracted from traces recorded without the inhibitor. Trace a–b: wild type; traces c–d: $\gamma\text{Met23Lys}$ mutant. The continuous lines are obtained by best fit of bi-exponential functions to the data. The initial rates were 134 and $88 \text{ mol ATP} \times \text{mol Bechl}^{-1} \times \text{s}^{-1}$ for pseudo-wild-type and $\gamma\text{Met23Lys}$ mutant, respectively. The inset shows an enlarged view of the same data.

113 preparations the vesicle size was larger (~60 nm) and each vesicle presumably
114 contained several ATP synthase molecules. Bacteriochlorophyll concentration was
115 determined in acetone-methanol extract at 772 nm according to [42].

116 2.2. Introduction of the γ Met23Lys mutation

117 Plasmid pRCAT1 was constructed from the plasmid pRCA50 (carrying the
118 *Rb. capsulatus* F₁ operon inserted in pTZ18R [43]) by cutting the latter with
119 EcoRI and ligating the 7.6-kb fragments with T4 DNA ligase.

120 The mutation was introduced into the pRCAT1 plasmid by using the
121 QuickChange Site-Directed Mutagenesis Kit (Stratagene), using the following
122 oligonucleotides for the PCR: 5'-CAAGATCACGAAAGCGAAGCA-
123 GATGGTCGCGG-3' and 5'-GTTCTAGTGCTTCGCTTCGTCTAC-
124 CAGCGCC-3'. Successful introduction was confirmed by restriction analysis
125 with *HpyCH4V* restriction endonuclease, which produced a 1600-bp fragment in
126 the mutated plasmid instead of ~900 bp, ~700 bp, and smaller fragments in the
127 pRCAT1. The mutated F₁ operon was then cloned into the broad-host-range
128 plasmid pRK415 [44] carrying the tetracycline resistance, as described previously
129 [43]. The new plasmid was named pRCA51.23K and was subsequently introduced
130 into *Rb. capsulatus* B100 strain by triparental conjugation [45] as modified in [43].
131 By this procedure, the wild-type chromosomal copy of the F₁-operon was deleted,
132 and a kanamycin resistance cassette was introduced in its place by GTA (Gene
133 Transfer Agent) transfer [46] and simultaneously the pRCA51.23K was
134 introduced. A pseudo-wild-type strain was constructed in parallel by the same
135 procedure, which harboured the plasmid pRCA51 (carrying the wild-type F₁
136 operon) and a kanamycin-resistance cassette instead of the chromosomal F₁
137 operon; this strain was used as a wild-type F₀F₁ control throughout the work. No
138 major differences in the F₀F₁ properties between this pseudo-wild-type p51 strain
139 and the B 100 wild-type without plasmids were observed.

140 2.3. Flash-spectrophotometric measurements

141 Chromatophores were suspended in the standard medium that contained 20 mM
142 glycylglycine, 20 mM Na₂HPO₄, 100 mM potassium chloride or acetate, 5 mM
143 magnesium chloride or acetate, 2 mM K₄[Fe(CN)₆], 5 μ M 1,1'-dimethylferrocene,
144 and 200 μ M ADP. 2 mM KCN was present to ensure that no $\Delta\bar{\mu}_{\text{H}^+}$ was generated in
145 the darkness by cytochrome *c* oxidase; pH was 7.9. The final concentration of
146 bacteriochlorophyll in the cuvette was 10–15 μ M. Measurements were done at
147 room temperature.

148 The kinetic flash-spectrophotometer used to monitor the flash-induced
149 absorption changes was described previously [47]. Flash-induced changes in $\Delta\psi$
150 were monitored via electrochromic absorption band shift of carotenoid pigments
151 at 522 nm (see [34] and references therein). The electrochromic absorption band
152 shift was calibrated in millivolts of $\Delta\psi$ by imposing a K⁺ diffusion potential in the
153 presence of valinomycin as in [34]. According to the calibration, a single
154 saturating actinic flash (10 μ s full width at half-maximum) generated \approx 70 mV of
155 $\Delta\psi$. This value was lower than the corresponding flash-induced $\Delta\psi$ in the B10
156 *Rb. capsulatus* strain reported earlier [34] due to the higher ratio of
157 bacteriochlorophyll to the photosynthetic centers (\approx 60:1 and \approx 100:1 in B10
158 and B100, respectively).

159 Eight single traces recorded in the same sample were averaged to increase
160 the signal to noise ratio. During the averaging, the time interval between the
161 flashes was 12 s; it was long enough for the electrochromic signal to relax to its
162 pre-flash background level. Monitoring light was cut off between the flashes to
163 avoid additional excitation of the sample and $\Delta\bar{\mu}_{\text{H}^+}$ generation. Three flashes at
164 12 s interval were given to each sample before measurements to avoid any
165 effects of the longer than 12 s incubations in darkness.

166 Changes of the pH inside the chromatophores were monitored by
167 amphiphilic pH indicator neutral red [48] at 545 nm as in [34], but no bovine
168 serum albumin was present (changes in pH of the bulk phase were effectively
169 abolished by the pH buffers present). Nigericin, an electroneutral K⁺/H⁺
170 exchanger, was added to 1 μ M to quench the flash-induced pH changes [25,49].

171 2.4. Measurements of ATP hydrolysis

172 When ATP hydrolysis was measured with the colorimetric pH indicator Phenol
173 Red, chromatophores (10 μ M Bchl) were suspended in 0.5 mM Tricine, 1 mM

MgCl₂, 25 mM KCl, 0.2 mM succinate, 100 μ M Phenol Red, pH 8.0. The reaction
174 temperature was 25 °C. The cuvette was illuminated from above by a light guide
175 coming from a 250-W quartz-tungsten halogen lamp, filtered by a colored glass
176 long-pass filter with a cut-on wavelength of 780 nm. The pH changes of the
177 suspension were followed as a function of time by the absorbance changes at 625–
178 587 nm, and were calibrated after about 300 s of reaction by 3-fold addition of
179 25 μ M HCl. The overall pH change of the suspension at the end of the mea-
180 surements was never higher than 0.3 units. The changes of proton concentration
181 were transformed to changes of ATP concentration as described [50].
182

2.5. Measurements of ATP-driven proton pumping

183 ACMA fluorescence quenching assays were carried out in a Jasco FP 500
184 spectrofluorometer (wavelength 412 and 482 nm for excitation and emis-
185 sion respectively) at 25 °C. Chromatophores were suspended to 10 μ M
186 bacteriochlorophyll in the following buffer: 0.5 mM Tricine, 50 mM KCl,
187 2 mM MgCl₂, 1 mM NaPi, 0.2 mM succinic acid, NaOH to pH 8.0, an actinic
188 effect of the excitation beam was eliminated by adding as inhibitor of the
189 electron transport chain antimycin (5 μ M) and by attenuating the excitation
190 light by a 0.6 density filter (Ealing no. 35-5818); ACMA was added to
191 0.7 μ M. Prior to each measurement, the sample pH was adjusted to 8.0 with
192 NaOH. Final ATP concentration was 600 μ M. Measurements were done at
193 room temperature.
194

2.6. Measurements of ATP synthesis

195 The light-driven steady state ATP synthesis rate, as reported in Table 1, was
196 measured at 25 °C in the following buffer: 5 mM Tricine/NaOH, pH 8.0, 25 mM KCl,
197 1 mM MgCl₂, 2 mM Pi, 0.5 mM succinic acid, 10 μ M Bchl. The chromatophore
198 suspension was illuminated from one side by a 250-W Xenon lamp and from the
199 opposite side by a 150-W slide projector. The reaction was started by addition of
200 200 μ M ADP. After stopping the reaction at various times with 6% trichloroacetic acid,
201 the ATP concentration in each sample was measured in a luminometer (LKB 1250)
202 with the ATP-Monitoring Kit (Labsystems). The small amount of ATP synthesized in
203 the dark (due to the adenylate kinase reaction) was subtracted. The amount of
204 synthesized ATP was evaluated by adding 50–100 nM ATP.
205

206 ATP synthesis in response to the actinic flashes was measured as in [47].
207 Measuring medium was the same as in the flash-spectrophotometric experiments,
208 but 0.2 mM luciferin and 5–15 U/ml luciferase were present. For the mea-
209 surements of the flash-induced ATP synthesis and activation we used the same
210 Xenon arc flash as for the flash-spectrophotometric experiments. The photo-
211 multiplier (Thorn EMI 9256B, UK) was shielded against actinic light by a stack
212 of 3 blue filters (BG 39 Schott, Mainz, Germany). Measurements were done at
213 room temperature.

214 The luciferin–luciferase system was calibrated in each sample by addition
215 of freshly prepared ATP solution. The calibration was linear in the range of 0 to
216 5 μ M final ATP concentration. Slight decrease in the sensitivity (which became
217 more pronounced upon increase in the ATP concentration) during the
218 measurements was taken into account by repetitive calibrations during and
219 after each experiment. In the presence of ADP (without any ATP added) a
220 minor ATP synthesis (up to 10 fM/s per mM BChl) insensitive to F₀F₁
221 inhibitors was observed, probably due to adenylate kinase activity of
222 chromatophores. The latter activity resulted in increase of ATP concentration
223 to 400–700 nM.

Table 1

	ATP hydrolysis rate, no light, no uncouplers mmol ATP \times mol Bchl ⁻¹ \times s ⁻¹	ATP hydrolysis rate (30 s illumination, then light turned off and uncouplers added) mmol ATP \times mol Bchl ⁻¹ \times s ⁻¹	ATP synthesis rate, mmol ATP \times mol Bchl ⁻¹ \times s ⁻¹	t
Wild-type	13 \pm 3	134 \pm 14	175 \pm 7	t1.2
γ Met2Lys mutant	4 \pm 1	88 \pm 12	97 \pm 5	t1.3

224 3. Results

225 3.1. Activation of ATP hydrolysis by continuous illumination

226 It was demonstrated previously that $\Delta\tilde{\mu}_{\text{H}^+}^+$ activates ATP
 227 hydrolysis in *Rb. capsulatus* chromatophores [28]. The increase
 228 in the ATPase activity in response to $\Delta\tilde{\mu}_{\text{H}^+}^+$ is best observed
 229 when the membrane is first energized, and then uncoupled.
 230 Under such conditions the enzyme stays activated for some
 231 time, while the back-pressure of $\Delta\tilde{\mu}_{\text{H}^+}^+$ is relieved and does not
 232 limit the rate of ATP hydrolysis. This behavior was reproduced
 233 in the chromatophores with the wild-type F_0F_1 used in this
 234 work (Fig. 1, trace a). After 30 s of illumination, $\Delta\tilde{\mu}_{\text{H}^+}^+$ generated
 235 by photosynthetic proteins was dissipated by switching off the
 236 light and by simultaneous addition of the uncouplers (nigericin
 237 and valinomycin). At this point a high rate of ATP hydrolysis
 238 was observed, which then slowly decayed. Oligomycin, a specific
 239 inhibitor that binds to F_0 [51,52] and blocks the proton
 240 translocation [47], was used to confirm that this ATPase activity
 241 was coupled to proton transport through F_0 (Panel A, trace b, d
 242 in Fig. 1). To calculate the rate of the coupled ATP hydrolysis,
 243 the traces obtained with oligomycin were subtracted from the
 244 traces recorded without the inhibitor (panel B in Fig. 1). After
 245 subtraction of the oligomycin trace, the initial rate of hydrolysis
 246 amounted to $134 \text{ mM ATP} \times \text{M}^{-1} \text{ BChl} \times \text{s}^{-1}$ (Panel B, trace a–

b), and it decayed to the half after 28 s. The $\gamma\text{Met23Lys}$ mutant 247
 similarly showed a high initial rate of hydrolysis (88 mM 248
 $\text{ATP} \times \text{M}^{-1} \text{ BChl} \times \text{s}^{-1}$, Panel B, trace c–d), but the decay rate 249
 was markedly higher (half-life time 5 s). These data are 250
 summarized in Table 1, together with the ATP hydrolysis rates 251
 measured in the dark without pre-illumination and with ATP 252
 synthesis rates measured under continuous light as described in 253
 Materials and methods. The values of the rates were obtained 254
 after best fitting the original data points (see Fig. 1B). The 255
 transient high rate of hydrolysis observed in the M23K mutant, 256
 although decaying very rapidly, was consistently reproduced in 257
 different preparations. This observation suggests that the 258
 mutated ATPase can indeed hydrolyse ATP efficiently, although 259
 the lifetime of its light-activated state is very short. This 260
 conclusion has been supported by further observations (de- 261
 scribed in Fig. 7, see below). It is also interesting to note that 262
 while the activated wild-type hydrolysis rate was 10-fold higher 263
 than the non-activated rate, the mutant rate was activated by a 264
 factor of 22 (see Table 1). 265

3.2. Effect of $\gamma\text{Met23Lys}$ mutation on the flash-induced proton 266 transport through F_0F_1 267

The results described above (Fig. 1 and Table 1) indicated 268
 that $\gamma\text{Met23Lys}$ F_0F_1 efficiently catalyzed ATP synthesis; the 269

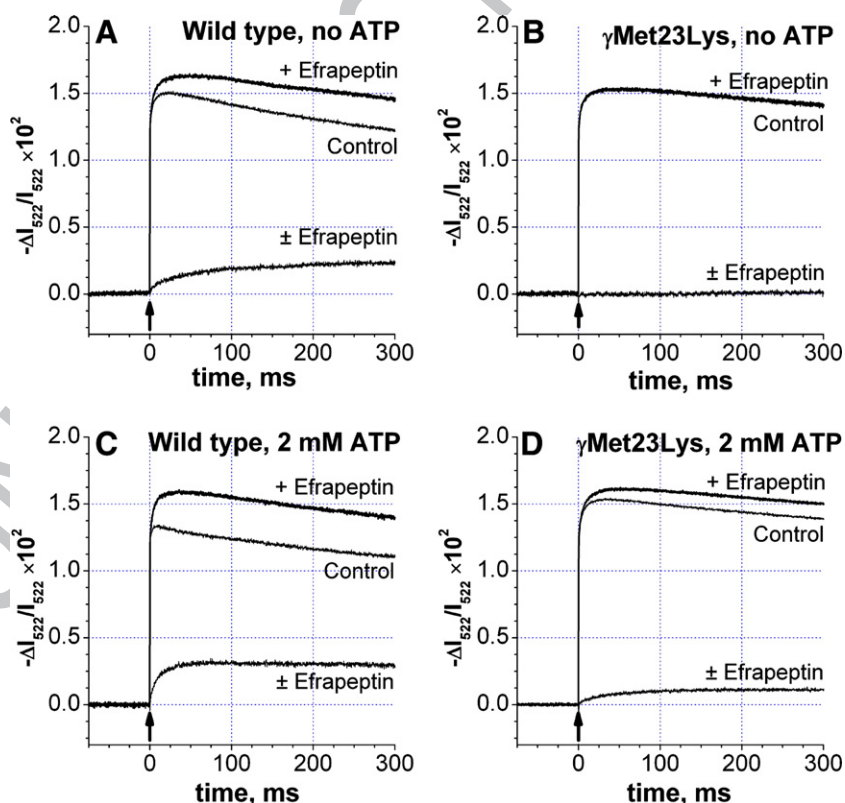


Fig. 2. Flash-induced electrochromic traces recorded at 522 nm in the wild-type and $\gamma\text{Met23Lys}$ mutant chromatophores. Medium contained 20 mM glycylglycine, 20 mM Na_2HPO_4 , 100 mM KCl, 5 mM MgCl_2 , 2 mM KCN, 2 mM $\text{K}_4[\text{Fe}(\text{CN})_6]$, 5 μM 1,1'-dimethylferrocene, and 200 μM ADP; pH was 7.9. In panels C and D, 2 mM ATP was present. After recording the *Control* trace, efrapeptin was added to final concentration of 200 nM. *Efrapeptin* trace was recorded 3 min after the addition of the inhibitor. $\pm\text{Efrapeptin}$ trace was obtained by subtracting the *Control* trace from the *Efrapeptin* trace. Bacteriochlorophyll concentration was 15 μM . Actinic flashes are indicated by arrows. Each trace is an average of 8 individual traces recorded at 12-s interval in the same sample.

270 ATPase activity of the mutant enzyme was sensitive to F_O-
 271 inhibitor oligomycin and was stimulated by $\Delta\tilde{\mu}_{\text{H}}^+$. These find-
 272 ings imply that the coupling between F_O and F₁ was not lost,
 273 so we decided to investigate the proton translocation in the
 274 γ Met23Lys mutant under ATP synthesis conditions using short
 275 flash of light for membrane energization. The excitation of *Rb.*
 276 *capsulatus* chromatophores by a single saturating actinic flash
 277 results in fast generation of $\Delta\tilde{\mu}_{\text{H}}^+$ across the chromatophore
 278 membrane (see [47] and the references therein for a detailed
 279 description of the flash-induced generation of the $\Delta\tilde{\mu}_{\text{H}}^+$ in *Rb.*
 280 *capsulatus* chromatophores).

281 This voltage generation can be monitored by electrochromic
 282 carotenoid absorption band shift at 522 nm, as shown in Fig. 2
 283 and as described in Materials and methods. Absorbance changes
 284 at this wavelength are proportional to the changes in $\Delta\psi$ (see
 285 [34] and references therein), which in turn are proportional to
 286 the net charge transfer across the membrane.

287 The biphasic rise of the $\Delta\psi$ is followed by decay due to various
 288 ion fluxes including proton transport through the F_OF₁. The
 289 component of $\Delta\psi$ decay reflecting the proton escape from
 290 chromatophore vesicles can be obtained by recording traces with
 291 and without specific inhibitors and by calculating the respective \pm
 292 inhibitor difference trace. To determine the coupled proton trans-
 293 port we have used efrapeptin, a peptide antibiotic that binds
 294 inside F₁ between subunit γ and $\alpha_3\beta_3$ hexamer [53,54], whereas
 295 oligomycin has been used to estimate the total (coupled and
 296 uncoupled) proton transport. It was shown previously that the
 297 efrapeptin-sensitive component of $\Delta\psi$ decay correlates with
 298 proton uptake from the chromatophore interior and proton release
 299 into the bulk medium [34,55,56]. It was also shown that the extent
 300 of this $\Delta\psi$ decay component quantitatively correlates with ATP
 301 synthesis [47]. Thus, for the sake of simplicity below we refer
 302 to the \pm efrapeptin traces as to “coupled proton transport”.

303 Fig. 2 illustrates the flash-induced $\Delta\psi$ changes and the coupled
 304 proton transport in chromatophores with wild-type F_OF₁ and with
 305 the γ Met23Lys mutant enzyme. In correspondence with the
 306 results obtained previously [47], in chromatophores with the wild-
 307 type F_OF₁ a single flash in the presence of ADP and phosphate led
 308 to coupled proton transport of considerable extent (Fig. 2A). The
 309 data in Fig. 2 indicate that its maximal extent in the wild-type
 310 chromatophores was \approx 15% of the total flash-induced charge
 311 transfer (compare traces \pm Efrapeptin and \pm Efrapeptin). In con-
 312 trast to the wild-type chromatophores, there was no detectable
 313 coupled proton transport under the same conditions in case of
 314 γ Met23Lys mutant (Fig. 2B). Oligomycin also had no effect in
 315 γ Met23Lys, ruling out insensitivity to efrapeptin as a possible
 316 effect of the γ Met23Lys mutation (not documented).

317 When ATP was present at the final concentration of 2 mM,
 318 the coupled proton transport increased both in the wild-type and
 319 in the mutant (Fig. 2, panels C and D). The relative increase
 320 induced by ATP was much smaller in the wild-type sample. It
 321 should be noted that as the chromatophores had on average less
 322 than one active ATP synthase per vesicle, changes in the extent
 323 of the coupled proton transport reflected changes in the fraction
 324 of active enzyme [34,35]. So the increase observed was likely
 325 due to activation rather than to change in the turnover rate of
 326 active enzyme.

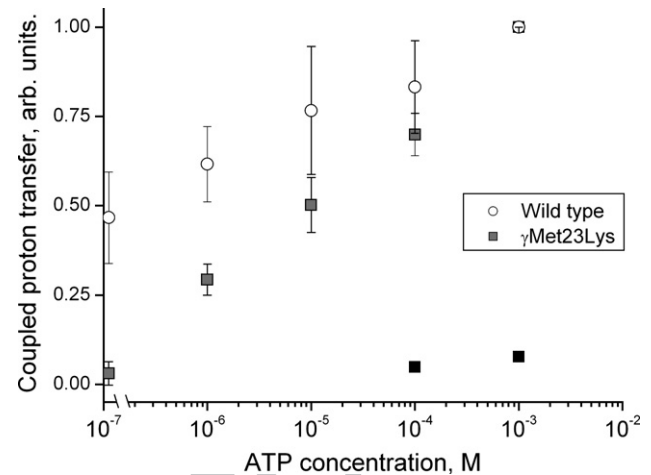


Fig. 3. Dependence of the extent of the flash-induced coupled proton transport through F_OF₁ on ATP concentration. Measuring medium was as in Fig. 2. Open circles—wild-type (strain p51) chromatophores; closed grey squares— γ Met23Lys chromatophores; closed black squares— γ Met23Lys chromatophores, but AMP-PNP was added instead of ATP. The extent of the \pm Efrapeptin difference trace (see Fig. 2) was divided by the extent of the flash-induced electrochromic response of the photosynthetic reaction centres; the value at 1 mM ATP was taken as unity. At least three experiments were made for each ATP concentration. Standard error is plotted as bars.

327 To further characterize the effect, we investigated the de-
 328 pendence of the extent of the flash-induced coupled proton
 329 transport on ATP concentration (Fig. 3). It should be noted
 330 that even when no ATP was added to the sample, there was
 331 still some (\approx 0.5 μ M) ATP present due to the contamination
 332 in ADP and to the adenylate kinase activity of chromato-
 333 phores. Elimination of this residual ATP by glucose and
 334 hexokinase further diminished the extent of the flash-induced
 335 coupled proton transport in the wild-type enzyme (not
 336 documented).

337 A marked increase in the relative extent of the coupled proton
 338 transport with increase in ATP concentration was clear both in
 339 the wild-type and in the mutant γ Met23Lys enzyme (Fig. 3). In
 340 contrast to ATP, 1 mM AMP-PNP (a non-hydrolysable ATP
 341 analogue) failed to increase the extent of the coupled proton
 342 transport, indicating that not mere ATP binding, but ATP
 343 hydrolysis was necessary for the effect observed.

344 The results obtained were in apparent contradiction with
 345 thermodynamic considerations: increase in the concentration of
 346 the reaction product (ATP) was supposed to suppress rather than
 347 stimulate the reaction. However, it was in good agreement with
 348 the proposed above facilitated inactivation of the γ Met23Lys
 349 mutant enzyme. We found probable that the $\Delta\tilde{\mu}_{\text{H}}^+$ generated by
 350 ATP hydrolysis during the dark adaptation time between the
 351 flashes could hinder this inactivation.

352 To validate this hypothesis we increased in the wild-type the
 353 dark adaptation time between the flashes during the trace
 354 averaging to provide more time for deactivation. The data
 355 presented in Fig. 4 indicate that the extent of the flash-induced
 356 coupled proton transport declined to zero upon the increase of
 357 the time interval between the flashes. The time constant of
 358 deactivation was \approx 10 s and was significantly higher than the

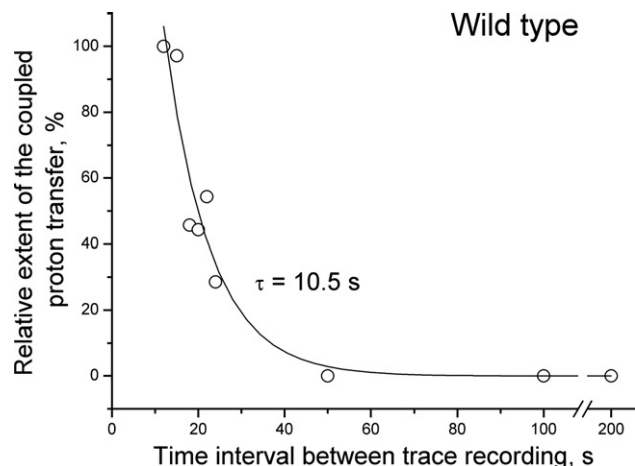


Fig. 4. Dependence of the extent of the flash-induced coupled proton transport in the wild-type *Rb. capsulatus* chromatophores on the interval between the flashes. Measuring medium was as in Fig. 2. Traces were averaged at different time interval (12–200 s, depicted on the x-axis). The relative extent of the \pm Efrapeptin difference trace was taken as a measure of the coupled proton flow through F_0F_1 ; the extent of the trace averaged at 12-s interval was taken as

359 time constant of $\Delta\psi$ decay (<3 s). This observation suggested
 360 that the difference between the wild-type and the γ Met23Lys
 361 F_0F_1 was merely in accelerated inactivation of ATP hydrolysis

in the mutant, where no flash-induced coupled proton transport 362
 was detected even at shortest interval (12 s) between the 363
 flashes. 364

3.3. Activation of ATP hydrolysis at low ATP/ADP ratio 365

To further clarify the role of γ Met23Lys mutation in the 366
 deactivation of F_0F_1 , and to investigate the $\Delta\mu_{H^+}$ activation of 367
 ATP hydrolysis by short flashes of light, we measured the flash- 368
 induced ATP synthesis and the subsequent ATP hydrolysis. A 369
 series of 1–20 flashes at 60 ms interval were given, and the 370
 concomitant ATP synthesis/hydrolysis were monitored by 371
 luciferin-luciferase system. The concentration of ATP before 372
 the actinic flashes was ≈ 1 μ M; ADP concentration was 200 μ M. 373
 As can be seen in Fig. 5 (panels A and C), in the wild-type 374
 chromatophores the rate of ATP hydrolysis, while negligible after 375
 one flash, increased markedly with the increase in the number of 376
 flashes. In contrast, in the γ Met23Lys mutant (panels B and D) 377
 even a series of 20 flashes did not activate ATP hydrolysis, 378
 although considerable flash-induced ATP synthesis was 379
 observed. 380

The yield of ATP synthesized per flash in 20-flash series was 381
 similar in the wild-type and in the γ Met23Lys mutant: $0.173 \pm$ 382
 0.035 mmol ATP \times mol $^{-1}$ BChl per flash for the wild-type and 383
 0.206 ± 0.066 mmol ATP \times mol $^{-1}$ BChl per flash for the 384

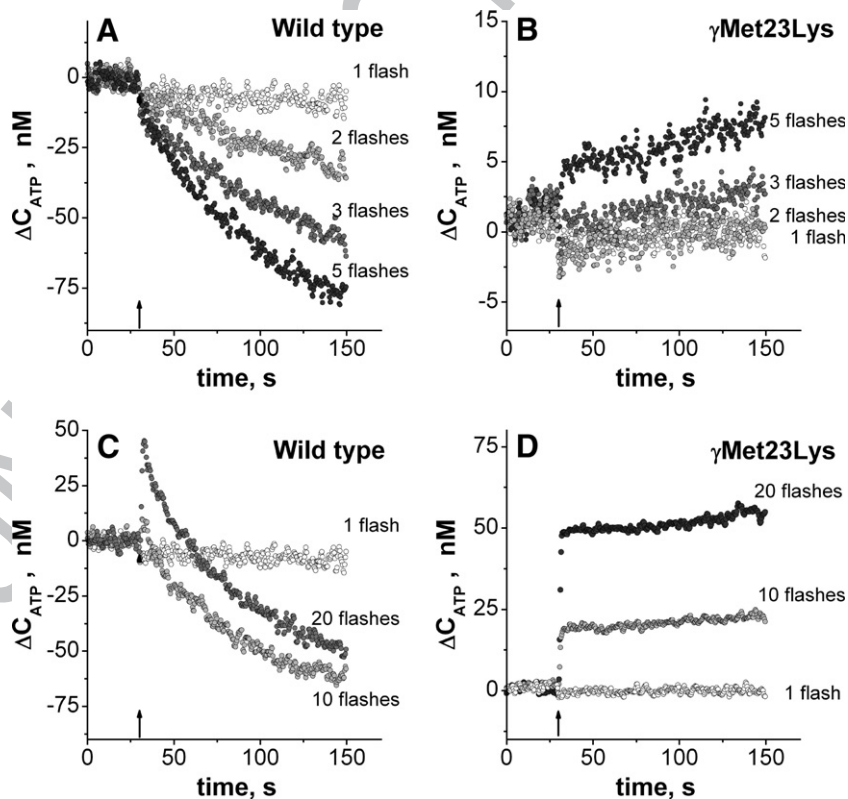


Fig. 5. Flash-induced ATP synthesis and activation of ATP hydrolysis in chromatophores of *Rb. capsulatus* wild-type and γ Met23Lys mutant. Changes in ATP concentration were monitored by luciferin–luciferase as indicated in Materials and methods. ATP concentration was ≈ 1 μ M. Traces were corrected for the background linear shift present before the flash series. Note the different scale on y-axis. Each trace was recorded after at least 2 min dark adaptation. Bacteriochlorophyll concentration was 18 μ M in the wild-type sample and 15 μ M in the γ Met23Lys mutant sample. A—wild-type, 1–5 flashes; B— γ Met23Lys, 1–5 flashes; C—wild-type, 1–20 flashes; D— γ Met23Lys, 1–20 flashes.

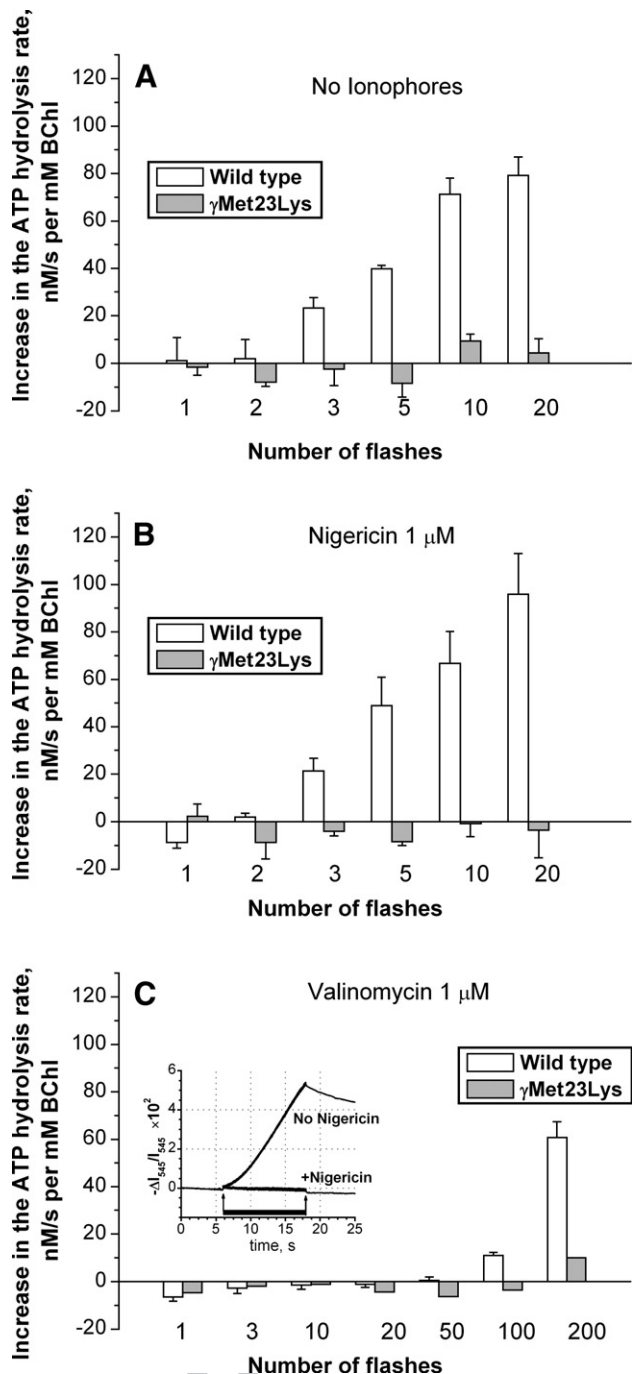


Fig. 6. Activation of the ATP hydrolysis by flash-induced $\Delta\mu_{H^+}$. The activation was measured as absolute increase in the initial rate of ATP hydrolysis (measured by luciferin–luciferase as in Fig. 5) after the series of actinic flashes. At least three measurements were done for each flash series (standard error plotted on each column). (A) No uncouplers. (B) 1 μ M nigericin present. (C) 1 μ M valinomycin present. The inset in panel C illustrates the generation of $\Delta\mu_{H^+}$ during the 200-flash series and absence of $\Delta\mu_{H^+}$ generation when 1 μ M nigericin was present (1 μ M valinomycin was present in both experiments). The $\Delta\mu_{H^+}$ was monitored by neutral red at 545 nm as described in Materials and methods. The flash series is indicated by black bar with arrows.

385 γ Met23Lys mutant. This result indicated that the lower coupled
 386 proton transport observed in γ Met23Lys mutant chromatophores
 387 was not due to lower expression level of the enzyme.

3.4. The role of $\Delta\psi$ and $\Delta\mu_{H^+}$ in the activation of ATP hydrolysis 388

To assess the individual role of the electrical and the chemical components of $\Delta\mu_{H^+}$ in the activation of *Rb. capsulatus* F_0F_1 under the experimental conditions used, valinomycin and nigericin were applied to selectively quench $\Delta\psi$ or $\Delta\mu_{H^+}$, respectively. As a measure of the activation, the difference between the rate of ATP hydrolysis before and after the flash series was taken. As can be seen in panels A and B in Fig. 6, no major changes in the extent of activation of the wild-type enzyme occurred upon quenching of $\Delta\mu_{H^+}$ by 1 μ M nigericin. This result was in good correspondence with earlier study reporting a negligibly small value of $\Delta\mu_{H^+}$ generated in *Rb. capsulatus* chromatophores after a single flash in the presence of a pH-buffer glycyglycine [49]. A control experiment with the amphiphilic pH indicator neutral red confirmed the latter data (not documented).

When the flash-induced $\Delta\psi$ was abolished by 1 μ M valinomycin, no detectable activation was observed even after a series of 50 flashes (Fig. 6C). However, increase in the flash number to 100 or 200 resulted in considerable acceleration of the ATP hydrolysis. It should be noted that a small residual absorption change at 522 nm was observed in response to flash series even in the presence of valinomycin (5–15% of the signal recorded in the absence of valinomycin; not documented). Therefore it cannot be excluded that some residual $\Delta\psi$ (<30 mV) was generated under such conditions.

Control experiments with amphiphilic pH indicator neutral red (Fig. 6C, inset) revealed that with such a high number of flashes a substantial $\Delta\mu_{H^+}$ was generated even in the presence of 20 mM glycyglycine and 20 mM phosphate. This result might indicate that $\Delta\mu_{H^+}$ could also efficiently contribute to the activation of ATP hydrolysis in the wild-type enzyme. Once again, no activation was observed in the γ Met23Lys mutant (although some small degree of activation after 200 flashes cannot be excluded).

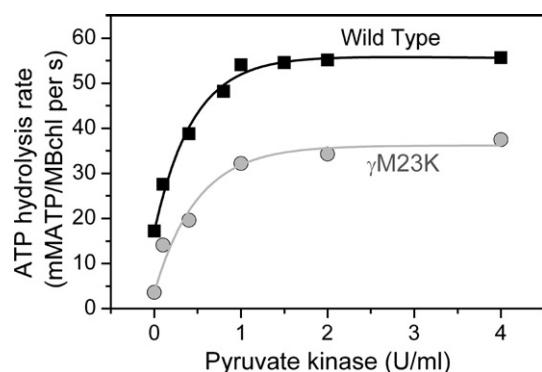


Fig. 7. Dependence of the ATPase activity in the wild-type and γ Met23Lys mutant chromatophores on the concentration of pyruvate kinase. Measuring medium contained: tricine 10 mM, KCl 50 mM, $MgCl_2$ 4 mM, succinic acid 0.2 mM, lactate dehydrogenase 25 U/ml, KCN 2.5 mM, PEP 2 mM, NaP_i 1 mM, Antimycin 5 μ M, NADH 0.15 mM, ATP 0.6 mM. In the measurements with no pyruvate kinase ATPase activity was measured by phenol red assay in tricine 1 mM, P_i 1 mM, KCl 50 mM, $MgCl_2$ 4 mM, Succinic acid 0.2 mM, phenol red 100 μ M. In all experiments pH was 8.0. Chromatophores were added to final concentration of 10 μ M bacteriochlorophyll.

The data presented in Fig. 6 show that a single flash was not enough to achieve full activation of ATP hydrolysis in the wild-type chromatophores, indicating a relatively high $\Delta\mu_{\text{H}}^+$ threshold for activation. Measurements of electrochromic absorption changes induced by a series of flashes revealed that the maximal $\Delta\psi$ value under repetitive flash excitation at 16.7 Hz (60 ms interval) was ≈ 170 mV and that it was reached after 5–6 flashes. The higher extent of the F_0F_1 activation upon the increase in the flash number from 5 to 10 and 20 indicated that the activation was a slow process and required relatively long (i.e. hundreds of milliseconds) exposure to $\Delta\mu_{\text{H}}^+$.

The results presented in Fig. 6 indicated that the activation of ATP hydrolysis by $\Delta\mu_{\text{H}}^+$ could not be detected in the γ Met23Lys mutant under all the experimental conditions used (20 mM phosphate, 200 μ M ADP, 1 μ M ATP, and flash induced activation).

3.5. Activation of the hydrolysis by an ATP regenerating system

The inhibition of the ATPase by MgADP is a well established phenomenon in all ATP synthases and also in F_1 (see [57] and the references therein). Auto- and photoactivation of the ATPase in *Rb. capsulatus* chromatophores [28] can be related to the release of inhibitory ADP, consistent with the direct demonstration of this mechanism in the chloroplast enzyme [24]. In line with this view, the addition of the pyruvate kinase (PK) /phospho-enol pyruvate (PEP) ADP trap that strongly reduces free ADP in the assay medium induced a stimulation of the hydrolysis rate in wild-type chromatophores (Fig. 7). Additions of increasing amounts of PK, thereby producing a progressively smaller concentration of ADP during the reaction, progressively stimulated the hydrolysis rate to a maximum asymptotic value.

Similar behavior was apparent in chromatophores from γ Met23Lys mutant, although the reaction rates were systematically lower at all PK concentrations tested. However, the difference in the ATP hydrolysis rate of the wild-type and mutant F_0F_1 measured in the absence of ATP regenerated system was approximately fourfold, but only ~ 1.5 -fold in the presence of the latter

(Table 1; Fig. 7). This result indicated that inhibition by ADP was enhanced in the γ Met23Lys mutant.

The ATP hydrolysis measured in the wild-type in the absence of PK in Fig. 7 was 17 ± 3 mmol ATP \times mol Bchl⁻¹ \times s⁻¹ (average of 3 determinations). The higher value relative to that reported in Table 1 was due to the presence of 1 mM P_i, which is known to slightly stimulate the ATP hydrolysis in *Rb. capsulatus* (see e.g. (58)). On the contrary, no effect of P_i could be detected in the activity of the mutant enzyme, which was 4 ± 1 mmol ATP \times mol Bchl⁻¹ \times s⁻¹ (average of 3 determinations).

In these measurements, a kinetically limiting PK concentration can be excluded since, even at the lowest concentration, its activity was in about 20-fold excess relative to the ATP hydrolysis activity.

3.6. ATP-driven proton pumping in the γ Met23Lys mutant

It was reported previously that in *E. coli* ATP synthase the introduction of the γ Met23Lys mutation severely impairs the coupling efficiency and leads to a complete loss of ATP-driven proton pumping [40]. In contrast, earlier measurements from the same group reported only a partial decrease in the coupling efficiency, and detectable (although markedly reduced) ATP-driven proton pumping [58].

Our results suggested that in *Rb. capsulatus* the mutant was coupled, as deduced from the oligomycin sensitivity of ATP hydrolysis and high ATP synthesis rate. To directly address this issue, we measured the ATP driven proton pumping in the wild-type and γ Met23Lys chromatophores by the ACMA assay. As can be seen in Fig. 8, the mutant enzyme was active in proton pumping, although the initial rate was lower than in the wild-type. In all cases the ACMA quenching induced by ATP was completely reversed by 0.5 μ M nigericin (Fig. 8).

This result confirmed that in *Rb. capsulatus* ATP synthase the γ Met23Lys did not abolish the ATP driven proton pumping under the experimental conditions used.

In an attempt to improve the comparison between the coupling efficiency of the γ Met23Lys and of the wild-type F_0F_1 , the rate of ATP hydrolysis in the wild-type enzyme was inhibited with 125 nM efrapeptin to a level observed in the non-inhibited mutant sample. Under these conditions the pumping rate in the two strains was very similar, suggesting that the reduced rate observed in the mutant was caused by lower hydrolysis rate rather than by lower efficiency of coupling.

4. Discussion

4.1. The γ Met23Lys mutation does not affect the coupling efficiency in *Rb. capsulatus* F_0F_1

Previously the effects of γ Met23Lys mutation were extensively studied in *E. coli* F_0F_1 . The mutation was found to slightly reduce the ATPase activity [36,37] and to impair markedly (although not completely) the coupling between ATP hydrolysis and proton pumping [58]. Another study reported a complete loss of the coupling [40]. Surprisingly, in single molecule experiments the mutated F_1 was shown to generate

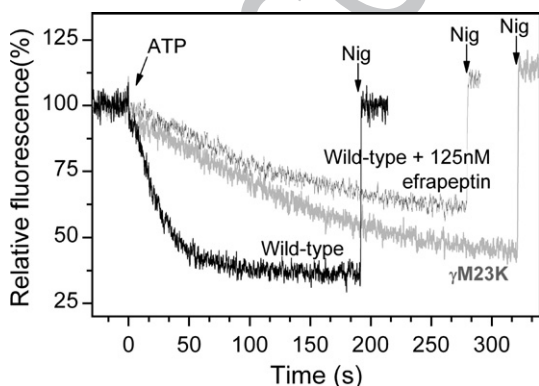


Fig. 8. ATP-driven proton pumping in the wild-type chromatophores, in the γ Met23Lys chromatophores, and in the wild-type chromatophores partially inhibited by 125 nM efrapeptin (so that the ATPase activity matched that of the uninhibited mutant sample). Chromatophores were suspended to 20 μ M Bchl in 1 mM Tricine, 50 mM KCl, 4 mM MgCl₂, 1 mM NaP_i, 0.2 mM succinic acid, pH 8.0; ACMA was added to 0.75 μ M. Additions of ATP (600 μ M) and of nigericin (500 nM) are indicated by arrows.

509 the same torque during ATP-driven rotation, and the rotation
510 speed was also indistinguishable from those of the wild-type F_1
511 [40].

512 Our results indicated that in *Rb. capsulatus* the γ Met23Lys
513 mutation altered the activity of F_0F_1 in several ways. The most
514 obvious effect was a more than threefold decrease in the rate of
515 non-activated ATP hydrolysis (Fig. 1, Table 1, Fig 7). In
516 contrast, ATP synthesis activity was only moderately impaired
517 (less than two-fold under steady-state conditions, see Table 1).
518 The enzyme also performed considerable ATP-driven proton
519 pumping and no marked difference in the coupling efficiency
520 was detected between the wild-type and the mutant enzyme
521 (Fig. 8). Moreover, the data in Fig. 2 indicate that no proton
522 transport took place through the mutant enzyme in the presence
523 of ADP and phosphate (although some efrapeptin-sensitive
524 transport was readily observed after addition of ATP). These
525 results confirmed that the mutant enzyme was not intrinsically
526 “leaky” to protons. Absence of leaks in the entire membrane
527 was also previously documented for the *E. coli* γ Met23Lys
528 mutant, by examining the proton pumping induced by lactate
529 respiration [58].

530 A comparison of the amino acid sequences of the two enzymes
531 demonstrates that the γ subunits are very conserved between the
532 two bacteria: 115 over 290 amino acids are identical and most
533 non-identical residues have similar hydrophobicity and charge of
534 the side chain. The homology is even stricter for the β subunits
535 that exhibit 69% identity and 81% similarity. It is likely, therefore,
536 that our results with *Rb. capsulatus* can be compared with a good
537 degree of confidence to those obtained with *E. coli* ATP synthase,
538 although, in principle, a different behavior between the two
539 bacterial species cannot be excluded.

540 It is also conceivable that the uncoupling effects observed in
541 *E. coli* γ Met23Lys mutant were caused not by mutation itself,
542 but by the specific experimental conditions used in these
543 studies. Recent work on *Rb. capsulatus* F_0F_1 showed that the
544 presence of ADP and phosphate, and possibly $\Delta\tilde{\mu}_H^+$, is critically
545 important for efficient coupling [59]. The contrast between a
546 complete lack of ATP-driven proton pumping in *E. coli*
547 γ Met23Lys mutant reported in [40] and clearly detectable
548 (although small) proton pumping reported earlier in the same
549 strain [58] also suggests that experimental conditions, but not
550 γ Met23Lys mutation per se, caused uncoupling. As discussed
551 below, ADP concentration variations might have especially
552 strong influence on γ Met23Lys F_0F_1 activity.

553 4.2. Effect of γ Met23Lys mutation on the activation of ATP 554 hydrolysis by $\Delta\tilde{\mu}_H^+$

555 The results presented in Fig. 1 and Table 1 indicated that
556 activation of ATP hydrolysis by $\Delta\tilde{\mu}_H^+$ was present both in the
557 wild-type and in the mutant. The relative activation of the
558 coupled ATP hydrolysis after illumination was even higher in
559 the mutant (Table 1). However, the deactivation occurring after
560 uncoupling was markedly faster in the γ Met23Lys F_0F_1 (half-
561 time ≈ 5 s versus ≈ 25 s in the wild-type; Fig. 1).

562 Flash-induced coupled proton transport through the mutant
563 F_0F_1 also differed from that in the wild-type enzyme. The data in

Fig. 2 indicated that there was no detectable transport in
 γ Met23Lys chromatophores unless ATP was added to the sample.
However, upon addition of ATP the extent of the transport through
 F_0F_1 increased. This effect was also observed in the wild-type
chromatophores, but in the mutant the relative increase was much
higher.

The drop in the extent of the coupled proton transport indicated
a decrease in the fraction of vesicles having an active enzyme
[35,47], presumably due to the deactivation of the F_0F_1 . So the
results in Figs. 2 and 3 suggested that ATP prevented the
deactivation. Absence of such effect in case of AMP-PNP, a non-
hydrolysable ATP analogue (Fig. 3, dark closed squares), indicated
that not merely ATP binding, but hydrolysis was necessary.

A probable cause for the effect observed would be ATP-driven
generation of $\Delta\tilde{\mu}_H^+$. In this case the second and subsequent flashes
would have increased the $\Delta\tilde{\mu}_H^+$ not from zero, but from a relatively
high level determined by the phosphate potential (protonmotive
force of ≈ 100 mV could be expected under the experimental
conditions used with $1 \mu\text{M}$ ATP present and H^+/ATP ratio of 3.3).
According to the calibration with K^+ diffusion potential (data not
shown), a single flash generated ≈ 70 mV $\Delta\psi$ both in the wild-type
(strain p51) and in the γ Met23Lys mutant chromatophores. This
value was well below the thermodynamic threshold for ATP
synthesis. However, if this 70 mV was a surplus to a 100-mV
background that corresponded to the phosphate potential before the
flash, a considerable ATP synthesis would be expected.

This hypothesis was in good agreement with the observed
decrease of the flash-induced coupled proton transport upon
increase in the time interval between the flashes (Fig. 4). The
magnitude of the flash-induced $\Delta\tilde{\mu}_H^+$ was approximately the
same irrespective of the dark adaptation time, but the flash-
induced coupled proton transport declined to zero upon increase
in the interval. This indicated that in the dark the enzyme
gradually lost the ability to perform coupled proton transport.

The data in Fig. 2A (recorded with 12 s dark adaptation
before actinic flash) demonstrated that flash-induced coupled
proton transport occurred in the wild-type chromatophores with
no ATP added (i.e. the concentration of ATP was below $1 \mu\text{M}$).
In the framework of the rationale above, this implied that a
considerable fraction of the wild type F_0F_1 remained active 12 s
after the actinic flash even in the absence of added ATP. On the
contrary, in γ Met23Lys chromatophores a negligibly small
coupled proton transport indicated that the deactivation was
markedly faster. This result correlated well with the steady-state
ATP hydrolysis data that also confirmed a facilitated and
accelerated deactivation of the mutant enzyme after the actinic
illumination was turned off (Fig. 1).

The results presented in Fig. 5 demonstrated that in contrast to
the wild-type, at low ATP concentration (and high ADP
concentration) the activation of ATP hydrolysis could not be
detected at all in the mutant. It was also evident that no increase
in the ATP hydrolysis rate was observed in γ Met23Lys even in
the very first seconds after the actinic flashes. Since the mutant
enzyme did show high flash-induced ATP synthesis, indicating a
highly active state, the most likely conclusion is that the mutant
ATP synthase was deactivated immediately upon decrease of
 $\Delta\tilde{\mu}_H^+$ below the thermodynamic threshold of ATP synthesis.

621 Taken together, our results demonstrate that γ Met23Lys
622 mutation accelerated the transition from active to inactivated
623 state of F_0F_1 , most evidently at high ADP/ATP ratios.

624 4.3. γ Met23Lys mutation might stabilize the ADP-inhibited 625 state of the enzyme

626 The ~~deactivation~~ caused by tight binding of MgADP at one
627 of the F_0F_1 catalytic sites is a well-established mechanism of
628 ~~the enzyme regulation~~ [14–21]. It is also demonstrated that
629 upon the energization of the membrane the tightly bound ADP
630 is released from the F_1 -portion [20,22–25], that presumably
631 leads to the $\Delta\tilde{\mu}_H^+$ activation of the enzyme.

632 Recent experiments revealed that mechanic rotation of
633 subunit γ by 40° in the hydrolysis direction can also relieve
634 the ADP-inhibition in F_1 [60]. Preliminary data reported in the
635 latter work indicated that rotation of subunit γ by 160° in the
636 synthesis direction had the same effect. Without forced rotation
637 the spontaneous re-activation from the ADP-inhibited state is
638 induced by thermal rotational fluctuations of subunit γ , and is
639 completely blocked if the angular position of subunit γ is fixed
640 by external force [60].

641 It was suggested from the experiments on *E. coli* F_0F_1 that
642 impaired activity in γ Met23Lys mutant was due to electrostatic
643 interaction of the γ Lys23 with the first glutamate in the
644 β DELSEED fragment [39]. It is possible that such interaction
645 hindered γ rotation and thereby stabilized the ADP-inhibited state
646 of the enzyme.

647 Consistent with this suggestion, ADP removal by the PEP/PK
648 ATP regenerating system caused significantly more pronounced
649 increase in the ATPase activity of *Rb. capsulatus* γ Met23Lys
650 mutant F_0F_1 (8-fold vs. 4-fold in the wild-type, Fig. 7). This
651 directly demonstrates that the inhibitory effect of ADP was
652 enhanced in the mutant. The prompt inactivation of ATP
653 hydrolysis in γ Met23Lys F_0F_1 after activation by $\Delta\tilde{\mu}_H^+$ (Fig. 1),
654 and the nearly undetectable ATP hydrolysis after trains of flashes
655 at low ATP/ADP ratio (Fig. 6) corresponded well with this
656 suggestion.

657 In view of these findings it should be noted that even small
658 variations in ADP concentration might have a pronounced effect
659 on the ATPase activity of γ Met23Lys F_0F_1 . Therefore, it might be
660 misleading to compare measurements of proton pumping with
661 ACMA fluorescence quenching done without ATP regenerating
662 system with measurements of ATPase activity done with such
663 system.

664 The interaction of γ Lys23 with the first glutamate in
665 β DELSEED seems probable according to the high-resolution
666 crystal structures of the F_1 -portion: the distance between the
667 side chains of these residues is 3.4–4.7 Å [2,61–65]. This
668 conclusion has recently got support from the structural study
669 of the bovine enzyme inhibited by ADP and azide and
670 resolved at 1.95 Å: azide stabilizes the inhibitory ADP in the
671 beta-DP site, preventing the release of the nucleotide and the
672 binding of phosphate [66]. Since ~~routinely all~~ crystals were
673 grown in the presence of azide (about 3 mM), ~~all~~ less resolved
674 structures showing an ADP binding site also contained non-
675 resolved inhibitory azide and λ corresponded ~~therefore~~ to the

ADP-inhibited conformation. The β -subunit with the DEL-
SEED located close to γ 23 residue bears the high-affinity
catalytic site occupied by tightly bound ADP. According to the
data obtained on the single molecule level, the angular position
of the γ -subunit in the ADP-inhibited state (presumably caught
in the crystal structures mentioned) differs by 40° from the
“ATP-waiting” state observed under low ATP concentration
[67]. This implies that the electrostatic interaction between
 γ Lys23 and the first Glu in the β DELSEED fragment is
sterically impossible in the “ATP-waiting” active state. It
might be that in the γ Met23Lys enzyme the lifetime of the
active “ATP-waiting” state is reduced due to stabilization of
the γ -subunit angular position that corresponds to the ADP-
inhibited state.

The impaired $\Delta\tilde{\mu}_H^+$ activation in the γ Met23Lys mutant might
also be responsible for the discrepancy between the pronounced
effects of the mutation in the biochemical experiments and the
absence of any detectable effect on the ATP-driven torque
generation in the single-molecule rotational assays done on
E. coli F_1 [40]. As was mentioned above, ADP-inhibition blocks
the rotation of subunit γ [67], and spontaneous re-activation is
induced by stochastic rotational movement of the γ -subunit [60].
Therefore, stabilization of the ADP-inhibited state in the
 γ Met23Lys mutant proposed here would result merely in more
frequent and prolonged pauses of subunit γ rotation, but not in a
major decrease of the torque generated or of the turnover rate. As
long as the enzyme is not trapped in the ADP-inhibited state, it is
expected to perform ATP hydrolysis with the efficacy close to that
of the wild-type F_1 .

It should be noted that an alternative explanation for the
inhibitory effect of γ Met23Lys mutation was proposed by
Bandyopadhyay and Allison from the experiments on ther-
mophilic *Bacillus* PS3 $\alpha_3\beta_3\gamma$ complex. It was suggested that
not the electrostatic interactions, but disruption of a hydro-
phobic cluster located on subunit γ in the vicinity of the
 β DELSEED is responsible for impairment of catalysis [68].
However, since the mutation was shown to change the
activation energy for ATP hydrolysis [37], we still favor the
hypothesis of electrostatic interactions between γ Lys23 and
the first glutamate of the β DELSEED.

676 4.4. General conclusions on the activation of ATP hydrolysis 677 by $\Delta\tilde{\mu}_H^+$

678 Our results indicated that subunit γ plays a key role in the
679 activation of ATP hydrolysis by $\Delta\tilde{\mu}_H^+$. It seems likely that such
680 activation of F_0F_1 is merely a transition from the ADP-
681 inhibited state into active state caused by expelling of the
682 tightly-bound ADP from one of the catalytic sites. This ADP
683 release is most probably induced by the $\Delta\tilde{\mu}_H^+$ -driven rotation of
684 subunit γ . Our data point out that in *Rb. capsulatus* this rotation
685 could be driven either by pure $\Delta\psi$ or by Δ pH in the presence of
686 $\Delta\psi < 30$ mV. Electrostatic interactions of the negatively
687 charged β DELSEED fragment with γ Lys23 in the mutant
688 might stabilize the ADP-inhibited state and hinder subunit γ
689 rotation and therefore impair the activation of ATP hydrolysis
690 by $\Delta\tilde{\mu}_H^+$.

731 **Acknowledgments**

732 This research was supported by Deutsche Forschungsge-
733 meinschaft (grants DFG-SFB-431 and DFG-436-RUS-210), by
734 INTAS (nano-2001-736), and by the Italian Ministry of Education
735 and Research (MIUR) (PRIN Project “Bioenergetica e trasporto
736 in sistemi batterici e vegetali”, number 2005052128_004). B.A.F.
737 was supported by Alexander von Humboldt Foundation research
738 fellowship.

739 We would also like to thank Prof. Dr. Norbert Sewald and
740 Sven Weigelt from the University of Bielefeld for providing us
741 with efrapeptin C.

742 **References**

743 [1] R.A. Capaldi, B. Schulenberg, J. Murray, R. Aggeler, Cross-linking and
744 electron microscopy studies of the structure and functioning of the
745 *Escherichia coli* ATP synthase, *J. Exp. Biol.* 203 (2000) 29–33.
746 [2] C. Gibbons, M.G. Montgomery, A.G. Leslie, J.E. Walker, The structure of
747 the central stalk in bovine F₁-ATPase at 2.4 Å resolution, *Nat. Struct. Biol.*
748 7 (2000) 1055–1061.
749 [3] J.C. Greie, G. Deckers-Hebestreit, K. Altendorf, Subunit organization of
750 the stator part of the F₀ complex from *Escherichia coli* ATP synthase,
751 *J. Bioenerg. Biomembranes* 32 (2000) 357–364.
752 [4] R.H. Fillingame, W. Jiang, O.Y. Dmitriev, Coupling H⁺ transport to rotary
753 catalysis in F-type ATP synthases: structure and organization of the
754 transmembrane rotary motor, *J. Exp. Biol.* 203 (Pt 1) (2000) 9–17.
755 [5] T.M. Duncan, V.V. Bulygin, Y. Zhou, M.L. Hutcheon, R.L. Cross, Rotation
756 of subunits during catalysis by *Escherichia coli* F₁-ATPase, *Proc. Natl.*
757 *Acad. Sci. U. S. A.* 92 (1995) 10964–10968.
758 [6] H. Noji, R. Yasuda, M. Yoshida, K. Kinoshita Jr., Direct observation of the
759 rotation of F₁-ATPase, *Nature* 386 (1997) 299–302.
760 [7] D. Sabbert, S. Engelbrecht, W. Junge, Intersubunit rotation in active F-
761 ATPase, *Nature* 381 (1996) 623–625.
762 [8] R.A. Capaldi, R. Aggeler, Mechanism of the F₁F₀-type ATP synthase, a
763 biological rotary motor, *Trends Biochem. Sci.* 27 (2002) 154–160.
764 [9] J. Weber, A.E. Senior, ATP synthesis driven by proton transport in F₁F₀-
765 ATP synthase, *FEBS Lett.* 545 (2003) 61–70.
766 [10] P.D. Boyer, A research journey with ATP synthase, *J. Biol. Chem.* 277
767 (2002) 39045–39061.
768 [11] M. Yoshida, E. Muneyuki, T. Hisabori, ATP synthase—a marvelous rotary
769 engine of the cell, *Nat. Rev., Mol. Cell Biol.* 2 (2001) 669–677.
770 [12] R.K. Nakamoto, C.J. Ketchum, P.H. Kuo, Y.B. Peskova, M.K. al Shawi,
771 Molecular mechanisms of rotational catalysis in the F₀F₁ ATP synthase,
772 *Biochim. Biophys. Acta* 1458 (2000) 289–299.
773 [13] R.H. Fillingame, C.M. Angevine, O.Y. Dmitriev, Mechanics of coupling
774 proton movements to c-ring rotation in ATP synthase, *FEBS Lett.* 555 (2003)
775 29–34.
776 [14] C. Carmeli, Y. Lifshitz, Effects of P_i and ADP on ATPase activity in
777 chloroplasts, *Biochim. Biophys. Acta* 267 (1972) 86–95.
778 [15] A.F. Fitin, E.A. Vasilyeva, A.D. Vinogradov, An inhibitory high affinity
779 binding site for ADP in the oligomycin-sensitive ATPase of beef heart
780 submitochondrial particles, *Biochem. Biophys. Res. Commun.* 86 (1979)
781 434–439.
782 [16] I.B. Minkov, A.F. Fitin, E.A. Vasilyeva, A.D. Vinogradov, Mg²⁺-induced
783 ADP-dependent inhibition of the ATPase activity of beef heart mitochondrial
784 coupling factor F₁, *Biochem. Biophys. Res. Commun.* 89 (1979) 1300–1306.
785 [17] R.I. Feldman, P.D. Boyer, The role of tightly bound ADP on chloroplast
786 ATPase, *J. Biol. Chem.* 260 (1985) 13088–13094.
787 [18] J.M. Zhou, Z.X. Xue, Z.Y. Du, T. Melese, P.D. Boyer, Relationship of
788 tightly bound ADP and ATP to control and catalysis by chloroplast ATP
789 synthase, *Biochemistry* 27 (1988) 5129–5135.
790 [19] Y.M. Milgrom, P.D. Boyer, The ADP that binds tightly to nucleotide-
791 depleted mitochondrial F₁-ATPase and inhibits catalysis is bound at a
792 catalytic site, *Biochim. Biophys. Acta* 1020 (1990) 43–48.

[20] P. Fromme, P. Graber, Activation/inactivation and uni-site catalysis by the
793 reconstituted ATP- synthase from chloroplasts, *Biochim. Biophys. Acta*
794 1016 (1990) 29–42. 795
796 [21] I.Y. Drobinskaya, I.A. Kozlov, M.B. Murataliev, E.N. Vulfson, Tightly
797 bound adenosine diphosphate, which inhibits the activity of mitochondrial
798 F₁-ATPase, is located at the catalytic site of the enzyme, *FEBS Lett.* 182
799 (1985) 419–424. 800
801 [22] H. Strotmann, S. Bickel, B. Huchzermeyer, Energy-dependent release of
802 adenine nucleotides tightly bound to chloroplast coupling factor CF₁,
803 *FEBS Lett.* 61 (1976) 194–198. 804
805 [23] P. Graber, E. Schlodder, H.T. Witt, Conformational change of the chloroplast
806 ATPase induced by a transmembrane electric field and its correlation to
807 phosphorylation, *Biochim. Biophys. Acta* 461 (1977) 426–440. 808
809 [24] P. Sherman, M.J. Wimmer, Activation of ATPase of spinach coupling
810 factor 1. Release of tightly bound ADP from the soluble enzyme, *Eur. J.*
811 *Biochem.* 139 (1984) 367–371. 812
813 [25] B.A. Feniouk, A.Y. Mulikidjanian, W. Junge, Proton slip in the ATP
814 synthase of *Rhodobacter capsulatus*: induction, proton conduction, and
815 nucleotide dependence, *Biochim. Biophys. Acta* 1706 (2005) 184–194. 816
817 [26] W. Junge, Critical electric potential difference for photophosphorylation.
818 Its relation to the chemiosmotic hypothesis and to the triggering
819 requirements of the ATPase system, *Eur. J. Biochem.* 14 (1970) 582–592. 820
821 [27] B.A. Melandri, A. Baccarini-Melandri, E. Fabbri, Energy transduction in
822 photosynthetic bacteria. IV. Light-dependent ATPase in photosynthetic
823 membranes from *Rhodospseudomonas capsulata*, *Biochim. Biophys. Acta*
824 275 (1972) 383–394. 825
826 [28] P. Turina, B. Rumberg, B.A. Melandri, P. Graber, Activation of the H⁺-
827 ATP synthase in the photosynthetic bacterium *Rhodobacter capsulatus*,
828 *J. Biol. Chem.* 267 (1992) 11057–11063. 829
830 [29] S. Fischer, P. Graber, Comparison of Delta pH- and Delta phi-driven ATP
831 synthesis catalyzed by the H⁺-ATPases from *Escherichia coli* or
832 chloroplasts reconstituted into liposomes, *FEBS* 457 (1999) 327–332. 833
834 [30] M.A. Galkin, A.D. Vinogradov, Energy-dependent transformation of the
835 catalytic activities of the mitochondrial F₀F₁-ATP synthase, *FEBS Lett.*
836 448 (1999) 123–126. 837
838 [31] S. Fischer, P. Graber, P. Turina, The activity of the ATP synthase from
839 *Escherichia coli* is regulated by the transmembrane proton motive force,
840 *JBC* 275 (2000) 30157–30162. 841
842 [32] A.D. Vinogradov, T.V. Zharova, Energy-dependent transformation of
843 F₀F₁-ATPase in *Paracoccus denitrificans* plasma membranes, *J. Biol.*
844 *Chem.* 279 (2004) 12319–12324. 845
846 [33] J.B. Jackson, A.R. Crofts, The kinetics of light induced carotenoid changes
847 in *Rhodospseudomonas spheroides* and their relation to electrical field
848 generation across the chromatophore membrane, *Eur. J. Biochem.* 18
849 (1971) 120–130. 850
851 [34] B.A. Feniouk, M.A. Kozlova, D.A. Knorre, D.A. Cherepanov, A.Y.
852 Mulikidjanian, W. Junge, The proton driven rotor of ATP synthase: ohmic
853 conductance (10 fS), and absence of voltage gating, *Biophys. J.* 86 (2004)
854 4094–4109. 855
856 [35] B.A. Feniouk, D.A. Cherepanov, N.E. Voskoboynikova, A.Y. Mulikidjanian,
857 W. Junge, Chromatophore vesicles of *Rhodobacter capsulatus*
858 contain on average one F₀F₁-ATP synthase each, *Biophys. J.* 82 (2002)
859 1115–1122. 860
861 [36] M.K. al Shawi, C.J. Ketchum, R.K. Nakamoto, The *Escherichia coli* F₀F₁
862 gammaM23K uncoupling mutant has a higher K_{0.5} for P_i. Transition state
863 analysis of this mutant and others reveals that synthesis and hydrolysis
864 utilize the same kinetic pathway, *Biochemistry* 36 (1997) 12961–12969. 865
866 [37] M.K. al Shawi, R.K. Nakamoto, Mechanism of energy coupling in the F₀F₁-
867 ATP synthase: the uncoupling mutation, gammaM23K, disrupts the use of
868 binding energy to drive catalysis, *Biochemistry* 36 (1997) 12954–12960. 869
870 [38] M.K. al Shawi, C.J. Ketchum, R.K. Nakamoto, Energy coupling, turnover,
871 and stability of the F₀F₁ ATP synthase are dependent on the energy of
872 interaction between gamma and beta subunits, *J. Biol. Chem.* 272 (1997)
873 2300–2306. 874
875 [39] C.J. Ketchum, M.K. al Shawi, R.K. Nakamoto, Intergenic suppression of
876 the gammaM23K uncoupling mutation in F₀F₁ ATP synthase by betaGlu-
877 381 substitutions: the role of the beta380DELSEED386 segment in energy
878 coupling, *Biochem. J.* 330 (Pt 2) (1998) 707–712. 879
880

- 861 [40] H. Omote, N. Sambonmatsu, K. Saito, Y. Sambongi, A. Iwamoto-Kihara, 906
 862 T. Yanagida, Y. Wada, M. Futai, The gamma-subunit rotation and torque 907
 863 generation in F₁-ATPase from wild-type or uncoupled mutant *Escherichia* 908
 864 *coli*, Proc. Natl. Acad. Sci. U. S. A. 96 (1999) 7780–7784.
- 865 [41] J. Lascelles, Adaptation to form bacterichlorophyll in *Rhodospseudomonas* 910
 866 *sphaeroides*: changes in activity of enzymes concerned in pyrrole 911
 867 synthesis, Biochem. J. 72 (1959) 508–518.
- 868 [42] R.K. Clayton, Absorption spectra of photosynthetic bacteria and their 914
 869 chlorophylls, in: H. Gest, A. San Pietro, L.P. Vernon (Eds.), Bacterial 915
 870 Photosynthesis, The Antioch Press, Yellow Springs, OH, 1963, pp. 495–500.
- 871 [43] R. Borghese, M. Crimi, L. Fava, B.A. Melandri, The ATP synthase 916
 872 atpHAGDC (F₁) operon from *Rhodobacter capsulatus*, J. Bacteriol. 180 917
 873 (1998) 416–421.
- 874 [44] N.T. Keen, S. Tamaki, D. Kobayashi, D. Trollinger, Improved broad-host- 919
 875 range plasmids for DNA cloning in gram-negative bacteria, Gene 70 920
 876 (1988) 191–197.
- 877 [45] B.S. Sharak-Genthner, J.D. Wall, Ammonium uptake in *Rhodospseudo-* 922
 878 *monas capsulata*, Arch. Microbiol. 141 (1985) 219–224.
- 879 [46] M. Solioz, H.C. Yen, B. Marris, Release and uptake of gene transfer agent 924
 880 by *Rhodospseudomonas capsulata*, J. Bacteriol. 123 (1975) 651–657.
- 881 [47] B.A. Feniouk, D.A. Cherepanov, W. Junge, A.Y. Mulikidjanian, Coupling 925
 882 of proton flow to ATP synthesis in *Rhodobacter capsulatus*: F₀F₁-ATP 926
 883 synthase is absent from about half of chromatophores, Biochim. Biophys. 927
 884 Acta 1506 (2001) 189–203.
- 885 [48] W. Ausländer, W. Junge, Neutral red, a rapid indicator for pH changes in the 928
 886 inner phase of thylakoids, FEBS Lett. 59 (2) (1975) 310–315.
- 887 [49] A.Y. Mulikidjanian, W. Junge, Calibration and time resolution of luminal 929
 888 pH-transients in chromatophores of *Rhodobacter capsulatus* following a 930
 889 single turnover flash of light: proton release by the cytochrome bc₁- 931
 890 complex is strongly electrogenic, FEBS Lett. 353 (1994) 189–193.
- 891 [50] M. Nishimura, T. Ito, B. Chance, Studies on bacterial photophosphory- 932
 892 lation. III. A sensitive and rapid method of determination of photophos- 933
 893 phorylation, Biochim. Biophys. Acta 59 (1962) 177–182.
- 894 [51] P. Nagley, R.M. Hall, B.G. Ooi, Amino acid substitutions in mitochondrial 934
 895 ATPase subunit 9 of *Saccharomyces cerevisiae* leading to oligomycin or 935
 896 venturicidin resistance, FEBS Lett. 195 (1986) 159–163.
- 897 [52] M. Galanis, J.R. Mattoon, P. Nagley, Amino acid substitutions in 936
 898 mitochondrial ATP synthase subunit 9 of *Saccharomyces cerevisiae* 937
 899 leading to venturicidin or ossamycin resistance, FEBS Lett. 249 (1989) 938
 900 333–336.
- 901 [53] J.P. Abrahams, S.K. Buchanan, M.J. van Raaij, I.M. Fearnley, A.G. Leslie, 939
 902 J.E. Walker, The structure of bovine F₁-ATPase complexed with the peptide 940
 903 antibiotic cefrapeptin, Proc. Natl. Acad. Sci. U. S. A. 93 (1996) 9420–9424.
- 904 [54] P.E. Linnett, R.B. Beechey, Inhibitors of the ATP synthetase system, 941
 905 Methods Enzymol. 55 (1979) 472–518.
- [55] S. Saphon, J.B. Jackson, H.T. Witt, Electrical potential changes, H⁺ 906
 translocation and phosphorylation induced by short flash excitation in 907
Rhodospseudomonas sphaeroides chromatophores, Biochim. Biophys. 908
 Acta 408 (1975) 67–82.
- [56] B.A. Feniouk, D.A. Cherepanov, W. Junge, A.Y. Mulikidjanian, ATP- 910
 synthase of *Rhodobacter capsulatus*: coupling of proton flow through F₀ 911
 to reactions in F₁ under the ATP synthesis and slip conditions, FEBS Lett. 912
 445 (1999) 409–414.
- [57] B.A. Feniouk, T. Suzuki, M. Yoshida, The role of subunit epsilon in the 914
 catalysis and regulation of F₀F₁-ATP synthase, Biochim. Biophys. Acta 915
 1757 (2006) 326–338.
- [58] K. Shin, R.K. Nakamoto, M. Maeda, M. Futai, F₀F₁-ATPase gamma 917
 subunit mutations perturb the coupling between catalysis and transport, J. 918
 Biol. Chem. 267 (1992) 20835–20839.
- [59] P. Turina, D. Giovannini, F. Gubellini, B.A. Melandri, Physiological 919
 ligands ADP and P_i modulate the degree of intrinsic coupling in the ATP 920
 synthase of the photosynthetic bacterium *Rhodobacter capsulatus*, 921
 Biochemistry 43 (2004) 11126–11134.
- [60] Y. Hirono-Hara, K. Ishizuka, K. Kinoshita, M. Yoshida, H. Noji, Activation 922
 of pausing F₁ motor by external force, Proc. Natl. Acad. Sci. U. S. A. 102 923
 (2005) 4288–4293.
- [61] J.P. Abrahams, A.G. Leslie, R. Lutter, J.E. Walker, Structure at 2.8 Å resolution 924
 of F₁-ATPase from bovine heart mitochondria, Nature 370 (1994) 621–628.
- [62] K. Braig, R.I. Menz, M.G. Montgomery, A.G. Leslie, J.E. Walker, 925
 Structure of bovine mitochondrial F₁-ATPase inhibited by Mg²⁺ ADP and 926
 aluminium fluoride, Struct. Fold. Des. 8 (2000) 567–573.
- [63] R.I. Menz, J.E. Walker, A.G. Leslie, Structure of bovine mitochondrial F₁- 927
 ATPase with nucleotide bound to all three catalytic sites: implications for 928
 the mechanism of rotary catalysis, Cell 106 (2001) 331–341.
- [64] R.I. Menz, A.G. Leslie, J.E. Walker, The structure and nucleotide occupancy 929
 of bovine mitochondrial F₁-ATPase are not influenced by crystallisation at 930
 high concentrations of nucleotide, FEBS Lett. 494 (2001) 11–14.
- [65] R. Kagawa, M.G. Montgomery, K. Braig, A.G.W. Leslie, J.E. Walker, The 931
 structure of bovine F₁-ATPase inhibited by ADP and beryllium fluoride, 932
 EMBO J. 23 (2004) 2734–2744.
- [66] M.W. Bowler, M.G. Montgomery, A.G. Leslie, J.E. Walker, How azide 933
 inhibits ATP hydrolysis by the F₁-ATPases, Proc. Natl. Acad. Sci. U. S. A. 934
 103 (2006) 8646–8649.
- [67] Y. Hirono-Hara, H. Noji, M. Nishiura, E. Muneyuki, K.Y. Hara, R. Yasuda, 935
 K. Kinoshita Jr., M. Yoshida, Pause and rotation of F₁-ATPase during 936
 catalysis, Proc. Natl. Acad. Sci. U. S. A. 98 (2001) 13649–13654.
- [68] S. Bandyopadhyay, W.S. Allison, GammaM23K, gammaM232K, and 937
 gammaL77K single substitutions in the TF₁-ATPase lower ATPase activity 938
 by disrupting a cluster of hydrophobic side chains, Biochemistry 43 (2004) 939
 9495–9501.